

Transfer Learning Artificial Neural Network-based Ensemble Voting of Water Quality Classification for Different Types of Farming

Sumitra Nuanmeesri

Faculty of Science and Technology, Suan Sunandha Rajabhat University, Thailand
sumitra.nu@ssru.ac.th

Chaisri Tharasawatpipat

Faculty of Science and Technology, Suan Sunandha Rajabhat University, Thailand
chaisri.th@ssru.ac.th

Lap Poomhiran

Faculty of Science and Technology, Suan Sunandha Rajabhat University, Thailand
lap.po@ssru.ac.th (corresponding author)

Received: 16 May 2024 | Revised: 25 May 2024 | Accepted: 1 June 2024

Licensed under a CC-BY 4.0 license | Copyright (c) by the authors | DOI: <https://doi.org/10.48084/etasr.7855>

ABSTRACT

This study aims to develop a model for characterizing water quality in seawater-influenced areas for salt farming, fish farming, and crop farming. The water quality classification model was based on transfer learning trained by the Multi-Layer Perceptron Neural Network (MLPNN) and then classified by conventional Machine Learning (ML) methods, such as Decision Tree (DT), K-Nearest Neighbors (KNN), Logistic Regression (LR), Naive Bayes (NB), Random Forest (RF), and Support Vector Machine (SVM). The results of each ML classification were ensemble voted together, comparing the efficiency between hard and soft voting. The collected imbalanced dataset had a difference ratio between the majority and minority classes of 1:0.0138. However, after 900% resampling by applying the k-mean SMOTE technique, the data ratio between the majority and minority classes was 1:0.9778. The results show that the proposed ensemble approach improved accuracy by up to 2.15% in classifying water quality for salt farming, fish farming, and crop farming in seawater-influenced areas.

Keywords-artificial neural networks; transfer learning; ensemble voting; water quality classification

I. INTRODUCTION

The 71% of the Earth's surface is covered by water [1], with seawater making up the 97.5% of this total [2]. Seawater most likely affects areas close to or connected to the sea, as it invades freshwater sources, turning them into brackish water due to its salinity. In general, freshwater salinity levels are below 0.5 parts per thousand (ppt), in brackish water, they range from 0.5 to 30 ppt, and in saltwater, they exceed 30 ppt [3]. Although the distance between the coast and the river or canal is several kilometers apart, salinity inevitably permeates with the rhythm of the rising and falling tides. The most common solution is to install canal or sluice gates to prevent salinity and seawater [4-6]. Sometimes, these gates are scheduled to close and open, but most gates are manually operated [7]. In addition, some canals still constitute small boat routes for villagers and boat tours to visit various gardens and farms, so it is necessary to open the gate to facilitate water traffic. This inevitably causes freshwater to be converted to

brackish water, which directly affects farmers. Therefore, farmers in such areas must adapt and choose suitable occupations, mainly influenced by salinity. In some cases, different types of farming within the same area require different water salinity levels. For example, salt fields have an initial salinity requirement of 27-30 ppt [8]. Meanwhile, some fish, such as the Asian seabass (*Lates Calcarifer*), thrive in water with a salinity of 20 ppt [9]. At the same time, crop farms require little or very little water salinity, as salinity causes plants to wither or reduce yield [10, 11]. For this reason, the water sources in the vicinity for diverse farming operations affect the occupations of farmers. Sometimes, crop farms want to release freshwater to prepare for harvest. Freshwater released to the canal decreases the salinity of the fish farm, causing the fish to grow abnormally or unhealthy and then die. Therefore, a tool to classify water quality as suitable or not for different farms will help farmers prepare themselves to deal with or determine the appropriate time to close and open the sluice gates in the canal or river to adjust water quality.

In addition to water salinity, which is the main factor in areas adjacent to the coast or the sea, other factors that affect water quality, such as Electrical Conductivity (EC), Water Temperature (WT), and hydrogen potential (pH), have an impact on farming. These water quality parameters directly influence fish farms, since aquatic organisms have specific water quality requirements for breeding and growth. For example, pH shows how acidic or alkaline the water is [12]. However, high pH causes ammonia toxicity to increase, which is harmful to fish [13, 14]. Additionally, pH levels above 8.5 impact water's high carbonate and bicarbonate ion concentrations, affecting the nutritional balance of crops [15]. Higher pH also decreases plant root activity [16]. A 2°C increase in water temperature causes dehydration [17], as it concentrates water from fish excrement in cage-raised fish, which can harm them [18]. Moreover, fish will use more energy due to reduced Dissolved Oxygen (DO), affecting their growth rate [19].

Many studies have been conducted on water quality classification, including freshwater, brackish water, and seawater. Several studies applied ML algorithms to classify and predict the water quality index with high efficiency and stability [20]. Decision Tree (DT), Random Forest (RF), Logistic Regression (LR) [21], Naïve Bayes (NB), K-Nearest Neighbor (kNN), Support Vector Machine (SVM) [22], and Multi-Layer Perceptron Neural Network (MLPNN) are the most widely used ML algorithms for classifying water quality. However, these techniques are mainly used to benchmark models' performance. There are almost no studies that combine multiple machine-learning techniques in a single model to improve performance.

Today, technologies and systems are available to automatically collect different water quality data. The Internet of Things (IoT) is a technology that can connect to the network and upload data from hardware, such as sensors, to a cloud server. Therefore, this study developed a water quality IoT-based tool for collecting water quality data. Once developed, it will be installed in different areas to allow the system to automatically collect water quality data. Water quality data collection has become increasingly important for monitoring and protecting aquatic environments. Modern sensors and IoT devices have completely changed the way data are collected, as they can automatically measure crucial water parameters, including WT, EC, Chemical Oxygen Demand (COD), salinity, Biological Oxygen Demand (BOD), ammonia (NH₃), Total Suspended Solid (TSS), DO, pH, and turbidity. Through real-time monitoring, these devices can continuously read water quality data and transmit them wirelessly to a centralized data storage system. In this context, Google Sheets is an efficient and accessible platform for storing and managing collected data. By leveraging IoT technology and Google Sheets integration, water quality data can be effectively collected and analyzed, allowing researchers, environmentalists, and policymakers to make informed decisions and take prompt actions to ensure the sustainability and health of water resources.

This study explores the combination of several ML techniques, deploying MLPNN as the primary model for

feature extraction. The MLPNN model can be utilized as a transfer learning model. Additionally, six conventional ML methods, including DT, RF, LR, NB, kNN, and SVM, are followed to vote on the results to classify water quality as suitable for each farm type (fish, crop, and salt farms). The proposed method is expected to increase efficiency in classifying water quality by ensemble voting, as it contributes to better discrimination than the one performed when employing a single classifier. In addition, a focus group was held between researchers, community leaders, and farmers in Samut Songkhram province, who collaborated to develop a system and application to automatically collect water quality data from various sources in the research area to classify water quality suitability for the three types of farming. This system can be implemented to monitor and prevent losses due to poor water quality. Furthermore, users can find solutions to prevent and protect their farms in the developed application.

II. MATERIALS AND METHODOLOGY

Figure 1 presents the development of the model and the application developed to classify water quality for different farms using a transfer learning ANN-based ensemble voting technique, which consists of ten processes.

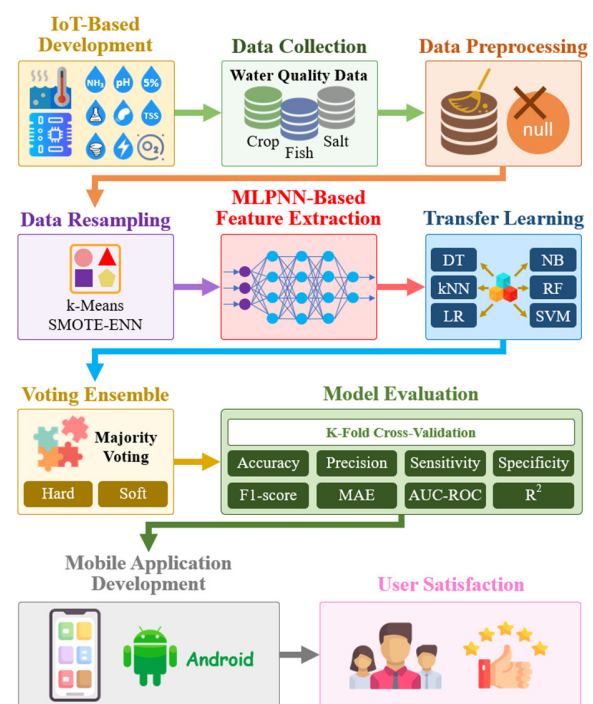


Fig. 1. The proposed research methodology.

A. IoT-based Development

IoT devices and sensors were designed and developed to automatically collect ten water quality parameters: WT, EC, salinity, NH₃, COD, BOD, TSS, pH, DO, and turbidity. This study employed the ESP32 DevKitC, which is a development board kit that can control smart sensors to measure water qualities. The versatility and low-power capabilities of ESP32

make it an ideal water-quality sensor integration, data acquisition, and wireless communication platform. It has 26 pins for General-Purpose Input/Output (GPIO) [23]. However, there is a limitation, as utilizing GPIOs directly with sensors whose pin combination exceeds the number of GPIOs available on the board is impossible. Therefore, this study applied the RS485 serial communication protocol with Modbus master and a maximum connection to 32 device-slaves. The ESP32 DevKitC was defined as master, and all water quality sensors were defined as slaves via the MAX485 chipset, which communicates to each sensor via the RS485 serial communication protocol.

The data read from the sensor are uploaded to Google Sheets deploying the Quectel EC21-E module allocated for 4G LTE in Thailand. The power supply to the system is generated by a 48-cell monocrystalline solar panel with a maximum voltage of 18 V and a maximum power of 300 W. Using Direct Current (DC) directly from the solar panel can cause problems. Thus, a 12 V 200 Ah deep cycle battery was put into service to supply power to the IoT system, which is charged through a solar charge controller with a Battery Management System (BMS) receiving the power directly from the solar panel. Some electronic devices require 5 V, so the LM2596 DC-DC step-down module was used to convert 12 V from the deep cycle battery to 5 V, and then supply the power for the MAX485 TTL to the RS485 module and ESP32 DevKitC board. The program to control the overall operation of the system was developed with Arduino IDE version 1.8.19 employing C++, as evidenced in Figure 2. Finally, the developed IoT-based water quality data collection systems were installed and deployed in the sample areas.

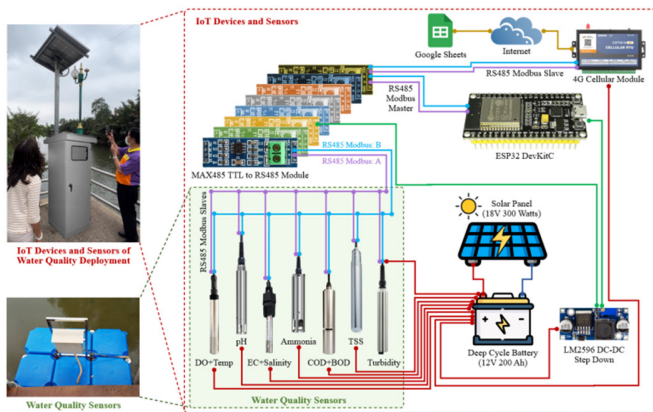


Fig. 2. The developed IoT-based system for water quality data collection.

B. Data Collection

In Thailand, three provinces have seaside areas and different farming activities (crop, fish, and salt farming): Samut Sakhon, Samut Songkhram, and Phetchaburi. All these provinces have similar spatial and geographic characteristics. Samut Songkhram covers the least area compared to the other two provinces. The research team chose Samut Songkhram as a prototype research area before expanding the storage and data collection area to cover the entire province and then expanding

the results to the other two provinces. The models obtained from these prototype study areas could be applied to the transfer learning model to nearby areas and provinces with similar geographical and occupational characteristics. Three sample areas were selected, covering diverse farms, to collect water quality data. The IoT systems developed to collect water quality parameters were deployed in three sample areas in the Don Manora, Phraek Nam Daeng, and Bang Kaeo subdistricts. In these subdistricts, the water flow routes cover different farms and are connected to the Gulf of Thailand. The Don Manora subdistrict focuses on crop farms, mainly growing vegetables and fruits. The Phraek Nam Daeng subdistrict is primarily involved in crop and fish farms or aquaculture. As the Bang Kaeo subdistrict is the closest to the coast, it mainly focuses on salt farming.

Water quality data were automatically collected by the aforementioned IoT system, scheduled to read and upload them to Google Sheets every hour, 24 hours a day, between 1 January and 30 June 2023 for the three subdistricts. The data collected totaled 13,040 records with ten water quality parameters: WT, pH, DO, EC, salinity, NH_3 , COD, BOD, TSS, and turbidity. However, since there may be cases where sensors malfunction and cannot measure or transfer data to the server, the data obtained were validated to ensure that they are as close as possible to reality. Any abnormal or unrelated data were eliminated in the data preprocessing process. Furthermore, during the collection of water quality data using the IoT, each week, some experts manually measured the water quality at each IoT kit location. This measured value was compared with the value obtained from the IoT kit to assess consistency. Any errors were checked and fixed to ensure that the IoT kit functioned normally. Additionally, the research team contacted community leaders and villagers in the research area to describe in detail the problems and importance of data collection and research procedures, as well as the ethical use of the model in research. All participants consented and signed to acknowledge ethics.

C. Data Preprocessing

Although the developed IoT system collected and uploaded data automatically, there were still uncertainties during the data storage process. For example, reading data errors due to abnormal sensor operation result in missing data or zero values, including duplicate data, causing re-uploading of the data if the system does not respond to the upload results. Cleaning up the data is a prerequisite. This process was performed using SQL to find duplicated and null items. Any record that matched the search condition was immediately deleted. After this process, 116 items were deleted, containing 8 duplicate and 108 missing value records, representing 0.89% of the data collected. Thus, the remaining data had a total of 12,924 records. Crop, fish, and salt farming experts were engaged in the class label assignment stage. The dataset included nine classes based on three different farm types and three severity levels: safe, warning, and critical. Table I depicts the class definitions and the amount of data.

D. Data Resampling

According to Table I, there is a varying amount of data between the majority class (3,417 records) and the minority

class (47 records), indicating an imbalanced dataset with an Imbalance Ratio (IR) of 72.70, as calculated by (1).

$$IR = \frac{\text{Amount of data in the majority class}}{\text{Amount of data in the minority class}} \quad (1)$$

This study applied the k-Means SMOTE-ENN to solve the imbalanced data problem. Since this dataset has ten input features, the k-cluster was set as $k = 5, 7, \text{ and } 9$ for the k-means clustering. The number of k-clusters was optimized using the scaled inertia method to find the cluster inertia for each k-cluster divided by the inertia of the first cluster (k_1). Scaled inertia can be calculated utilizing (2), (3), and (4) [24].

$$\text{Centroid}(k_i) = \frac{\sum_{j=1}^N x_j}{N} \quad (2)$$

$$\text{Inertia}(k_i) = \sum_{i=1}^N \|x_i - \text{Centroid}(k_i)\|^2 \quad (3)$$

$$\text{Scaled Inertia}(k_i) = \frac{\text{Inertia}(k_i)}{\text{Inertia}(k_1)} + \alpha \cdot k \quad (4)$$

where N denotes the data count in a cluster, x denotes the data in the cluster k_i , and α denotes the manually adjusted parameter that penalizes the clusters.

TABLE I. DETAILS OF THE CLASS DEFINITION

| Farming | Severity level | Class | Meaning | Amount of data |
|---------|----------------|-------|--|----------------|
| Crop | Safe | CS | The water quality is suitable and safe for growing fruits and vegetables. | 3,417 (26.44%) |
| Crop | Warning | CW | The water quality is beginning to tend to be unsuitable or unsafe for growing fruit and vegetables. | 1,618 (12.52%) |
| Crop | Critical | CC | The water quality is unsuitable for growing vegetables or fruits or is detrimental to the cultivated plants. | 363 (2.81%) |
| Fish | Safe | FS | The water quality is suitable for the growth of fish and aquaculture. | 1,839 (14.23%) |
| Fish | Warning | FW | The water quality is beginning to be unsuitable for fish growth and aquaculture. | 1,669 (12.91%) |
| Fish | Critical | FC | The water quality is inappropriate and harmful to fish growth and aquaculture. | 858 (6.64%) |
| Salt | Safe | SS | The water quality is suitable for salt production. | 2,471 (19.12%) |
| Salt | Warning | SW | The water quality tends to be unsuitable for salt production. | 642 (4.97%) |
| Salt | Critical | SC | The water quality is unsuitable and unsafe for salt production. | 47 (0.36%) |

After obtaining the ideal number of k-clusters, the dataset was processed through SMOTE for data resampling. The percentage of data oversampling was set ten times in increments of 100%, from 100% to 1000% for the SMOTE process, and the k-value. The count of nearest neighbors considered in the SMOTE and ENN process was set as k-nearest = 6, 8, and 10. Data increased according to the oversampling percentage. After completing the k-Means SMOTE-ENN process, the IR between the majority and

minority classes was close to one, and the dataset achieved class balance. In the end, 30 datasets differed between the percentage of data oversampling and the k-value of kNN. However, these datasets were subjected to simple DT classification and validated using 10-fold cross-validation to compare the difference in effectiveness obtained from several datasets. The dataset with the highest efficiency was implemented to further develop the proposed model.

E. MLPNN-based Feature Extraction

The MLPNN-based feature extraction was developed based on an ANN model having three layers: input, hidden, and output. The input layer has ten input features that correspond to the number of water quality parameters that are read by the sensors. The hidden layer has three Fully Connected (FC) layers for the MLPNN-based model, which are sufficient for feature extraction with a few features. Each FC layer contains hidden nodes, or neurons, that determine the rule of thumb based on the relationship between the number of input features and output classes. The number of hidden nodes for the first to the third of FC layers can be calculated by (5), (6), and (7), respectively.

$$\text{Nodes}(\text{Hidden}_1) = \left\lceil \left(\frac{2}{3}i\right) + c \right\rceil \quad (5)$$

$$\text{Nodes}(\text{Hidden}_2) = \left\lceil \frac{2}{3}(i + c) \right\rceil \quad (6)$$

$$\text{Nodes}(\text{Hidden}_3) = c \quad (7)$$

where i denotes the count of input features, and c denotes the count of output classes.

There are 10 input features and 9 output classes. Thus, each hidden layer has 16, 13, and 9 nodes, respectively. Each hidden layer applies bias nodes and the Rectified Linear Unit (ReLU) activation function due to their simplicity, effectiveness, and ability to promote faster training and improved convergence. Furthermore, a Batch Normalization (BN) layer followed each FC layer to normalize the activation and avoid overfitting. BN can help stabilize and accelerate the training process. Therefore, the hidden layer has six layers: three FC layers and three BN layers. The batch size was 64, and the training iteration was 500 epochs, with early stopping to prevent overfitting by monitoring the validation accuracy for patience, which was 50. The Adaptive moment estimation (Adam) optimizer was initialized with a learning rate of 0.01. There are 675 trainable parameters for the proposed MLPNN-based feature extraction model (excluding the output layer) and 765 trainable parameters for the MLPNN baseline model (including the output layer). Table II presents the hyperparameters for the MLPNN model.

The dataset was split into three sets, training, validation, and test, with a ratio of 60:20:20 using the random split with a stratified shuffle method to evenly distribute each class.

F. Transfer Learning

Upon completing the MLPNN-based feature extraction process, the resulting feature extraction was saved as the model. This learned model, with the extracted features, can be transferred to other models or classifiers as input features. Six conventional ML classifiers, DT, kNN, LR, NB, RF, and SVM,

were employed individually to classify water quality. Table III displays the hyperparameter configurations of each conventional ML classifier.

TABLE II. HYPERPARAMETERS OF THE MLPNN-BASED MODEL

| Hyperparameters | Details | No. of parameters |
|------------------------------|--|-------------------|
| Input layer | 10 nodes | 0 |
| 1st FC layer | 16 nodes, activation function:ReLU, bias (+1) | 176 |
| 1st BN layer | momentum=0.99, epsilon=0.0001 | 64 |
| 2nd FC layer | 13 nodes, activation function:ReLU, bias (+1) | 221 |
| 2nd BN layer | momentum=0.99, epsilon=0.0001 | 52 |
| 3rd FC layer | 9 nodes, activation function:ReLU, bias (+1) | 126 |
| 3rd BN layer | momentum=0.99, epsilon=0.0001 | 36 |
| Output layer (for baseline), | 9 nodes activation function:Softmax | 90 |
| Adam optimizer | learning rate = 0.01 | - |
| Batch size | 64 | - |
| Training iteration | 500 epochs, early stopping (monitor: validation accuracy, patience = 50) | - |

TABLE III. HYPERPARAMETERS OF THE MODELS

| Algorithm | Hyperparameters |
|-----------|--|
| DT | C4.5 algorithm, confidence level = 0.1, splitting criterion=Gini, random state = 42 |
| kNN | Distance metric = L2 norm, number of neighbors (k) = 5, 7, 9 |
| LR | L2 penalty = true, C-value = 1.0, max iterations = 100, tolerance = 0.001, random state = 42 |
| NB | Gaussian Naïve Bayes = true, log-space = 0 to -9 |
| RF | Estimators = 300 trees, batch size = 64, max depth = 0, max nodes = -1 (unlimited), bootstrapping = true, feature importance = Gini, random state = 42 |
| SVM | Kernel = Radial Basis Function (RBF), C-value = 1.0, gamma = 0.1, random state = 42 |

G. Ensemble Voting

The output class of each instant immediately received from each conventional ML model was collected and then voted using hard and soft voting. The efficiency of these voting and baseline models (DT with 10-fold cross-validation and MLPNN models) was compared. The ensemble hard-voting involves taking a majority vote from the predictions made by the individual base models. For classification tasks, the class labels predicted by each conventional ML model are counted, and then the class label acquiring the most votes is selected. The ensemble soft-voting considers the probabilities or confidence scores assigned by each base model, calculating the average probability for each class label on all models and then determining the ultimate prediction by selecting the class label with the highest average probability. After making predictions using the ensembles (hard or soft voting), the performance was evaluated on the test and validation datasets.

H. Model Evaluation

The performance of the proposed model was assessed utilizing accuracy, sensitivity, specificity, precision, F1-score,

Area Under the Curve of the Receiver Operating Characteristic (AUC-ROC) with balanced average accuracy [25], Mean Absolute Error (MAE) [26], and R-squared (R^2) [27]. Each metric was calculated as:

$$\text{Accuracy} = \frac{TP+TN}{TP+TN+FP+FN} \quad (8)$$

$$\text{Precision} = \frac{TP}{TP+FP} \quad (9)$$

$$\text{Sensitivity} = \frac{TP}{TP+FN} \quad (10)$$

$$\text{Specificity} = \frac{TN}{TN+FP} \quad (11)$$

$$\text{F1-score} = \frac{2 \times \text{Precision} \times \text{Sensitivity}}{\text{Precision} + \text{Sensitivity}} \quad (12)$$

$$\text{AUC-ROC} = \frac{\text{Sensitivity} + \text{Specificity}}{2} \quad (13)$$

where TP refers to the instances where the water quality is actually suitable and the model correctly identifies it as suitable, TN refers to the instances where the water quality is actually unsuitable and the model correctly identifies it as unsuitable, FP refers to the instances where the water is actually unsuitable but the model incorrectly identifies it as suitable, and FN refers to the instances where the water is actually suitable but the model incorrectly identifies it as unsuitable.

$$\text{MAE} = \frac{1}{N} \sum_{i=1}^N |y_i - \hat{y}_i| \quad (14)$$

where N denotes the count of observations of data, y_i denotes the true value, and \hat{y}_i denotes the expected value of data i .

$$R^2 = 1 - \left(\frac{\sum_{i=1}^N (x_i - \hat{x}_i)^2}{\sum_{i=1}^N (x_i - \bar{x}_i)^2} \right) \quad (15)$$

During the MLPNN-based model training, its categorical cross-entropy loss was calculated by:

$$\text{Cross-entropy Loss} = - \sum_{i=1}^x \sum_{j=1}^y z_{i,j} \log(p_{i,j}) \quad (16)$$

where x denotes the input data count, y denotes the count of classes, $z_{i,j}$ denotes the input data i corresponding to the class j , and $p_{i,j}$ denotes the expected value probability based on the class j by the input data i . In addition, a confusion matrix was used to evaluate the model's efficiency for comparing the accuracy of each predicted class.

I. Mobile Application Development

The model with the best performance results was developed on an Android-based mobile application platform deploying TensorFlow Lite and Android Studio version 2022.2.1 with C++. The developed application was based on Android version 7.0 (Nougat) with Application Programming Interface (API) version 24, which currently supports almost all Android platform devices. The mobile app can monitor the real-time water quality parameters by calling the web services API on the Apache Web Server and classifying the water quality. Figures 3 and 4 present the design of the mobile application's architecture and framework. In addition, five experts in information technology and computer science utilized the black-box testing methodology to assess the effectiveness of the mobile application. The consistency of the content in the

mobile application was evaluated employing an index of Item-Objective Congruence (IOC) [28, 29], with only three scores, including -1, 0, and 1. A score of 1 indicates that the expert accepted or agreed, while a score is 0 or -1 means the expert did not accept or disagreed [30]. The IOC is given by:

$$IOC = \frac{\sum_{i=1}^N \sum_{j=1}^M S_{i,j}}{N} \quad (17)$$

where N denotes the count of experts, M denotes the number of topics evaluated, and S denotes the score for each topic evaluated. This application was further distributed to farmers to test and evaluate user satisfaction.

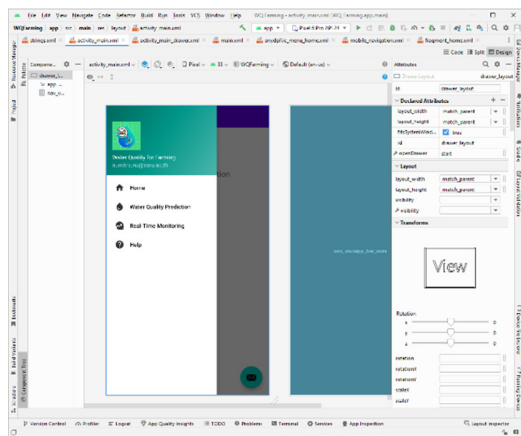


Fig. 3. The design of the mobile application in Android Studio.



Fig. 4. The architecture and framework of the mobile application.

J. User Satisfaction

Five experts in information technology or environmental sciences and thirty application users, who were farmers or villagers, attended training on using the developed system. All participants acknowledged, understood, and signed the ethics of the investigation. After completing the training process and demonstrating how to use the mobile application, users carried

out system tests to evaluate system performance based on user satisfaction. The evaluation score ranged in a five-point Likert scale [31]: 1 = very poor, 2 = poor, 3 = average, 4 = good, and 5 = excellent.

III. RESULTS AND DISCUSSION

A. Results of Data Resampling

Data resampling with the k-Means SMOTE-ENN method (100% to 1,000% of SMOTE) increased the amount of data from the original 12,954 records to 29,877 records. All minority classes were resampled to a number similar to the majority class. In addition, the imbalanced ratio was close to one, as observed in Figure 5. According to DT applying the 10-fold cross-validation on thirty datasets with k-means SMOTE-ENN for data resampling, the dataset configured with k-clusters = 9 and k-nearest = 8 had the highest accuracy. This dataset with 900% SMOTE had the highest accuracy of 84.77% and the imbalanced ratio was 1.0582, as exhibited in Figure 5.

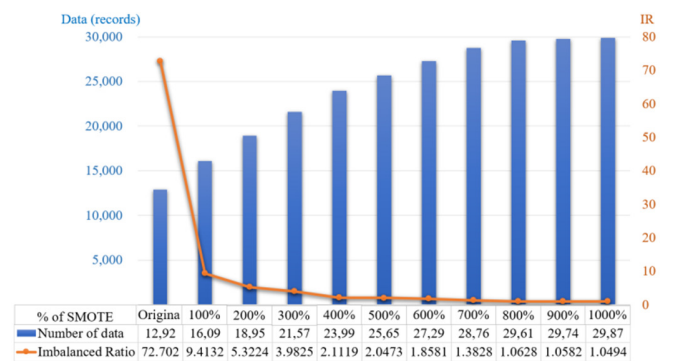


Fig. 5. The number of data resampled, imbalanced ratio, and dataset accuracy using k-means SMOTE-ENN (k-clusters = 9 and k-nearest = 8).

The dataset obtained for 1000% of SMOTE (29,877 records) was close to 900% of SMOTE (29,741 records), but the accuracy was slightly lower. This may be because the data were resampled in 100% increments, so the data with nine classes were resampled and all minority classes had a similar number to the majority class. Therefore, no additional data sampling is required. Many studies have solved the problem of imbalanced datasets using various techniques. Although the results give the model higher accuracy, resampling techniques are subject to biases and result in the tendency for the data to differ from the original data, failing to capture genuine data redundancy. Therefore, a comparison should be made with various techniques to manage imbalanced datasets to obtain techniques suitable for MLPNN-based models.

B. Results of Ensemble Voting

Feature extraction obtained from the MLPNN model was classified deploying conventional ML techniques with ensemble voting. The results reveal that the hard-voting model had the highest efficiency, with 86.62% accuracy, 86.64% precision, 87.25% sensitivity, 86.58% specificity, 87.04% F1-score, 86.76% AUC-ROC, 86.79% R², and 0.11064 MAE. The next best-performing models were the soft voting, MLPNN,

and DT (cross-validation) models, with accuracies of 86.59%, 85.25%, and 84.77%, respectively. In this regard, the DT (cross-validation) model was validated from the dataset attained from k-means SMOTE-ENN 900%, and the MLPNN model used the softmax activation function to classify classes without going through the ensemble voting process. Both models serve as a baseline to compare the results with the utilization of ensemble voting techniques, as disclosed in Figure 6.

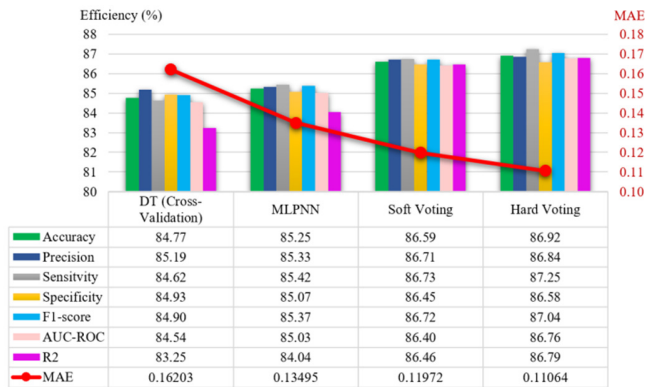


Fig. 6. Results of the ensemble voting compared with the baseline DT and MLPNN models.

The efficiencies of the hard- and soft-voting ensemble models had slight differences. The hard-voting model had a higher accuracy than the soft-voting one by 0.33%, while it had a higher accuracy of 1.67% and 2.15% compared to the MLPNN and DT models, respectively. Moreover, the sensitivity was progressively higher than the precision and higher than the accuracy for the hard voting model. However, MLPNN-based models with complex neural networks can limit the interpretability of the model. In addition, properly considering and optimizing the hyperparameters and related factors can help make the model more accurate.

C. Results of Mobile Application Development

The most efficient model was developed as a mobile application on the Android platform. Users can input individual water parameters to classify the severity level of water quality (warning, caution, and critical) of each farm type, as shown in the example application screen in Figure 7.

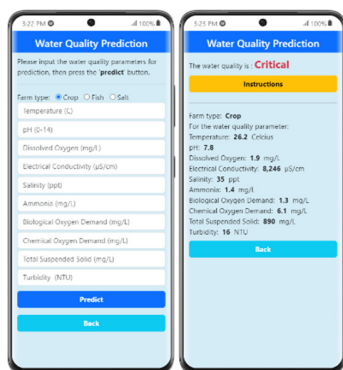


Fig. 7. The application of water quality classification for different farming.

D. Results on User Satisfaction

The average values of the user satisfaction evaluation were 4.96 for experts and 4.94 for farmers. Table IV indicates that the Standard Deviation (SD) values were 0.20 and 0.24 for experts and farmers, respectively. As shown in Table IV, the assessment topics 5, 7, and 8 had the highest mean score (5.00) for user satisfaction from experts and farmers. The assessment topics 1, 3, 4, 9, and 10, had a mean score of 5.00 when evaluated by experts, Meanwhile, the farmers' assessment had a lower mean than the experts' assessment, with a mean value of 4.90 for assessment topics no. 1, 3, and 4. For assessment topics 9 and 10, the mean value was 4.97. The assessment topics 2 and 6 received the lowest evaluation scores, having a mean value of 4.80 for experts and 4.83 and 4.90, respectively, for farmers. This may be due to small smartphone screens, causing the available space for display to decrease as well. Thus, a solution might be to divide the display into multiple pages so that filling out information and displaying information on each page has more space and does not cause the content to be too close together when the user uses a smartphone with a small screen.

TABLE IV. USER SATISFACTION ON THE MOBILE APPLICATION

| Assessment topics | Experts | | Users (Farmers) | |
|---|---------|------|-----------------|------|
| | Mean | SD | Mean | SD |
| 1. Font and text size | 5.00 | 0.00 | 4.90 | 0.31 |
| 2. Spacing between contents | 4.80 | 0.45 | 4.83 | 0.38 |
| 3. Ease of access menus | 5.00 | 0.00 | 4.90 | 0.31 |
| 4. Ease of access buttons | 5.00 | 0.00 | 4.90 | 0.31 |
| 5. Ease of use touch screen | 5.00 | 0.00 | 5.00 | 0.00 |
| 6. Contrast and appearance | 4.80 | 0.45 | 4.90 | 0.31 |
| 7. Vertical and horizontal screen orientation | 5.00 | 0.00 | 5.00 | 0.00 |
| 8. Help options | 5.00 | 0.00 | 5.00 | 0.00 |
| 9. Application performance | 5.00 | 0.00 | 4.97 | 0.18 |
| 10. The sense of familiarity | 5.00 | 0.00 | 4.97 | 0.18 |
| Average | 4.96 | 0.20 | 4.94 | 0.24 |

IV. CONCLUSION

Nearby areas may have farms that rely on water from the same source and are affected by seawater, especially the salinity value, which directly impacts different farming types with different salinity requirements. In addition, some water parameters directly affect water quality for farming. These parameters include water temperature, EC, salinity, ammonia, COD, BOD, TSS, pH, DO, and turbidity. This research presents guidelines for developing a mobile application for water quality classification for different farm types using MLPNN and voting ensemble-based conventional ML techniques, including DT, RF, LR, NB, kNN, and SVM. The dataset collected by IoT devices was resampled deploying the k-Means SMOTE-ENN to prevent overfitting caused by an imbalanced ratio between the majority and minority classes. A dataset with nine classes, processed with k-Means SMOTE-ENN at 900%, resulted in an imbalanced ratio close to one and the highest accuracy of 84.77% when validated with the DT 10-fold cross-validation. MLPNN was employed to extract features from the dataset, and then the output was classified using the softmax function. The MLPNN model had an

accuracy of 85.25%, higher than the baseline DT model. The features extracted from the MLPNN model were classified by six conventional ML algorithms and then voted utilizing hard and soft voting. The hard-voting model had higher efficiency than the soft-voting, MLPNN, and DT models. The accuracy was 86.92% and 86.59% for the hard and soft voting models, respectively. In addition, a smartphone application was developed to allow users to classify water quality following the hard voting approach. Farmers and experts were satisfied with the application, with means of 4.94 and 4.96, respectively.

In summary, developing a mobile application using transfer learning ANN-based ensemble voting can classify the water quality for different farming. The MLPNN-based model extracts features and then relies on several conventional classifiers to categorize the resulting classes and perform hard voting for the most accurate results. This method contributes to better discrimination than utilizing a single classifier. The value of this work is that farmers with different farm types have an application to predict water quality. This application can help farmers prevent and protect their farms, reduce yield loss from unsuitable water, and find ways to adjust water conditions to ensure that water quality is suitable for their farming operations. Although the model and system developed can help predict water quality, it can be expanded to an automatic water quality warning system to help farmers even more. However, this requires the cooperation of government agencies, community leaders, and those responsible for monitoring water quality and opening and blocking water gates. Therefore, sharing information and using various resources together is expected to help farmers earn a living and increase their income.

However, there may be some limitations to collecting water quality parameters with IoT and sensor devices via cellular networks. During automatic data collection, sensors can become fouled by algae, sediment, or biofilm, affecting the accuracy and performance of the measurements. Thus, these sensors need to be regularly cleaned and calibrated. Cellular network coverage may be poor in some areas, leading to unreliable data transmission. It is necessary to consider the installation location away from physical obstacles, as well as weather conditions and electromagnetic interference to have the most negligible impact on the quality and reliability of cellular networks. In addition, hyperparameters directly affect the efficiency of the proposed model. The hyperparameters of MLPNN and conventional classifiers must be tuned to achieve optimal performance. Water quality may change according to climate and season, including other external factors, such as industrial pollution, affecting the accuracy of the model. Thus, future research must consider all factors expected to be involved in water quality as input features and adopt feature selection methods to compare the efficiency of the models. Furthermore, this research only classifies water quality from the current water parameters. Therefore, a future work direction is to predict water quality in advance, using deep learning techniques, such as Deep Reinforcement Learning (DRL) and Recurrent Neural Networks (RNNs), and then combine their results with time series techniques to develop a model for classifying water quality near real-time and automatically

notify users. This can assist farmers and users plan water management more appropriately.

ACKNOWLEDGMENT

The authors express their gratitude to the Institute for Research and Development of Suan Sunandha Rajabhat University for their support and the opportunity to conduct this research. This research received support from the national budget for 2023, provided by Suan Sunandha Rajabhat University. The project was carried out under grant/contract number 11803/2566 with research ethics certificate number COE.1-039/2023.

REFERENCES

- [1] S. Y. Abuzir and Y. S. Abuzir, "Machine learning for water quality classification," *Water Quality Research Journal*, vol. 57, no. 3, pp. 152–164, May 2022, <https://doi.org/10.2166/wqrj.2022.004>.
- [2] R. K. Mishra, "Fresh Water availability and Its Global challenge," *British Journal of Multidisciplinary and Advanced Studies*, vol. 4, no. 3, pp. 1–78, May 2023, <https://doi.org/10.37745/bjmas.2022.0208>.
- [3] S. N. Surendran *et al.*, "Anopheline bionomics, insecticide resistance and transnational dispersion in the context of controlling a possible recurrence of malaria transmission in Jaffna city in northern Sri Lanka," *Parasites & Vectors*, vol. 13, no. 1, Mar. 2020, Art. no. 156, <https://doi.org/10.1186/s13071-020-04037-x>.
- [4] I. Ljubenkovic and S. Haddout, "Hydrodynamic modelling of a stratified estuary: the example of the Neretva River (Croatia)," *Marine Georesources & Geotechnology*, vol. 42, no. 1, pp. 14–25, Jan. 2024, <https://doi.org/10.1080/1064119X.2022.2147110>.
- [5] L. W. Morton, "Working toward sustainable agricultural intensification in the Red River Delta of Vietnam," *Journal of Soil and Water Conservation*, vol. 75, no. 5, pp. 109A–116A, Sep. 2020, <https://doi.org/10.2489/jswc.2020.0304A>.
- [6] L. Sriratana and K. Bisalyaputra, "Reconnaissance Study on Saltwater Intrusion Control at Main Raw Water Pumping Station of Metropolitan Waterworks Authority (Thailand)," *International Journal of Engineering and Technology*, pp. 33–38, Feb. 2019, <https://doi.org/10.7763/IJET.2019.V11.I1119>.
- [7] M. A. Ayaz, T. Manzoor, and A. Muhammad, "MPC Based Soil Moisture Regulation of a Canal-Connected Crop Field," *IFAC-PapersOnLine*, vol. 53, no. 5, pp. 170–175, Jan. 2020, <https://doi.org/10.1016/j.ifacol.2021.04.095>.
- [8] B. Kim *et al.*, "Aquavoltaic system for harvesting salt and electricity at the salt farm floor: Concept and field test," *Solar Energy Materials and Solar Cells*, vol. 204, Jan. 2020, Art. no. 110234, <https://doi.org/10.1016/j.solmat.2019.110234>.
- [9] H. U. Hassan *et al.*, "Growth performance and survivability of the Asian seabass *Lates calcarifer* (Bloch, 1790) reared under hyper-saline, hypo-saline and freshwater environments in a closed aquaculture system," *Brazilian Journal of Biology*, vol. 84, Mar. 2022, Art. no. e254161, <https://doi.org/10.1590/1519-6984.254161>.
- [10] B. E. Aydin, M. Rutten, G. H. P. O. Essink, and J. Delsman, "Polder Flushing: Model Predictive Control of Flushing Operations to Effective and Real Time Control of Salinity in Polders," *Procedia Engineering*, vol. 154, pp. 94–98, Jan. 2016, <https://doi.org/10.1016/j.proeng.2016.07.424>.
- [11] A. G. de Luna Souto *et al.*, "Salinity and Mulching Effects on Nutrition and Production of Grafted Sour Passion Fruit," *Plants*, vol. 12, no. 5, Jan. 2023, Art. no. 1035, <https://doi.org/10.3390/plants12051035>.
- [12] S. Jain and M. Kaur, "Design and Implementation of an IoT-based automated EC and pH Control System in an NFT-based Hydroponic Farm," *Engineering, Technology & Applied Science Research*, vol. 14, no. 1, pp. 13078–13081, Feb. 2024, <https://doi.org/10.48084/etasr.6393>.
- [13] A. J. Parvathy, B. C. Das, M. J. Jifiriya, T. Varghese, D. Pillai, and V. J. Rejish Kumar, "Ammonia induced toxico-physiological responses in fish

- and management interventions," *Reviews in Aquaculture*, vol. 15, no. 2, pp. 452–479, 2023, <https://doi.org/10.1111/raq.12730>.
- [14] F. Budiman, M. Rivai, and M. A. Nugroho, "Monitoring and Control System for Ammonia and pH Levels for Fish Cultivation Implemented on Raspberry Pi 3B," in *2019 International Seminar on Intelligent Technology and Its Applications (ISITIA)*, Surabaya, Indonesia, Aug. 2019, pp. 68–73, <https://doi.org/10.1109/ISITIA.2019.8937217>.
- [15] S. Chahal, S. K. Gautam, and P. R., "Hydrogeochemical Characterization and Assessment of Water Suitability for Irrigation in Salt-Affected Area of Israna block, Haryana, India," *Water Conservation Science and Engineering*, vol. 8, no. 1, Jun. 2023, Art. no. 20, <https://doi.org/10.1007/s41101-023-00194-z>.
- [16] G. Kaiwen *et al.*, "Effects of salt concentration, pH, and their interaction on plant growth, nutrient uptake, and photochemistry of alfalfa (*Medicago sativa*) leaves," *Plant Signaling & Behavior*, vol. 15, no. 20, Dec. 2020, <https://doi.org/10.1080/15592324.2020.1832373>.
- [17] H. A. Paltán, R. Pant, J. Plummer Braeckman, and S. J. Dadson, "Increased water risks to global hydropower in 1.5 °C and 2.0 °C Warmer Worlds," *Journal of Hydrology*, vol. 599, Aug. 2021, Art. no. 126503, <https://doi.org/10.1016/j.jhydrol.2021.126503>.
- [18] H. Li, Z. Cui, H. Cui, Y. Bai, Z. Yin, and K. Qu, "Hazardous substances and their removal in recirculating aquaculture systems: A review," *Aquaculture*, vol. 569, May 2023, Art. no. 739399, <https://doi.org/10.1016/j.aquaculture.2023.739399>.
- [19] S. Ayesha Jasmin, P. Ramesh, and M. Tanveer, "An intelligent framework for prediction and forecasting of dissolved oxygen level and biofloc amount in a shrimp culture system using machine learning techniques," *Expert Systems with Applications*, vol. 199, Aug. 2022, Art. no. 117160, <https://doi.org/10.1016/j.eswa.2022.117160>.
- [20] T. Yan, A. Zhou, and S.-L. Shen, "Prediction of long-term water quality using machine learning enhanced by Bayesian optimisation," *Environmental Pollution*, vol. 318, Feb. 2023, Art. no. 120870, <https://doi.org/10.1016/j.envpol.2022.120870>.
- [21] N. Nasir *et al.*, "Water quality classification using machine learning algorithms," *Journal of Water Process Engineering*, vol. 48, Aug. 2022, Art. no. 102920, <https://doi.org/10.1016/j.jwpe.2022.102920>.
- [22] S. Nuanmeesri, "A Hybrid Deep Learning and Optimized Machine Learning Approach for Rose Leaf Disease Classification," *Engineering, Technology & Applied Science Research*, vol. 11, no. 5, pp. 7678–7683, Oct. 2021, <https://doi.org/10.48084/etasr.4455>.
- [23] S. Nuanmeesri and L. Poomhiran, "Multi-Layer Perceptron Neural Network and Internet of Things for Improving the Realtime Aquatic Ecosystem Quality Monitoring and Analysis," *International Journal of Interactive Mobile Technologies (IJIM)*, vol. 16, no. 06, pp. 21–40, Mar. 2022, <https://doi.org/10.3991/ijim.v16i06.28661>.
- [24] O. Herman-Saffar, "An Approach for Choosing Number of Clusters for K-Means," *Medium*, Jun. 29, 2021. <https://towardsdatascience.com/an-approach-for-choosing-number-of-clusters-for-k-means-c28e614ecb2c>.
- [25] A. M. Carrington *et al.*, "Deep ROC Analysis and AUC as Balanced Average Accuracy, for Improved Classifier Selection, Audit and Explanation," *IEEE Transactions on Pattern Analysis and Machine Intelligence*, vol. 45, no. 1, pp. 329–341, Jan. 2023, <https://doi.org/10.1109/TPAMI.2022.3145392>.
- [26] W. Huo, W. Li, Z. Zhang, C. Sun, F. Zhou, and G. Gong, "Performance prediction of proton-exchange membrane fuel cell based on convolutional neural network and random forest feature selection," *Energy Conversion and Management*, vol. 243, Sep. 2021, Art. no. 114367, <https://doi.org/10.1016/j.enconman.2021.114367>.
- [27] A. S. Alkarim, A. S. A. M. Al-Ghamdi, and M. Ragab, "Ensemble Learning-based Algorithms for Traffic Flow Prediction in Smart Traffic Systems," *Engineering, Technology & Applied Science Research*, vol. 14, no. 2, pp. 13090–13094, Apr. 2024, <https://doi.org/10.48084/etasr.6767>.
- [28] R. J. Rovinelli and R. K. Hambleton, "On the use of content specialists in the assessment of criterion-referenced test item validity," presented at the Annual Meeting of the American Educational Research Association, San Francisco, CA, USA, Apr. 1976.
- [29] M. R. Lynn, "Determination and Quantification Of Content Validity," *Nursing Research*, vol. 35, no. 6, Dec. 1986, Art. no. 382.
- [30] S. Nuanmeesri, "Extended Study of Undergraduate Students' Usage of Mobile Application for Individual Differentiation Learning Support of Lecture-based General Education Subjects," *International Association of Online Engineering*, pp. 99–112, Sep. 2019, [Online]. Available: <https://www.learntechlib.org/p/216565/>.
- [31] R. Likert, "A technique for the measurement of attitudes," *Archives of Psychology*, vol. 22, No. 140, pp. 44–60, 1932.